Initial characterization of MPA CVD diamond to be investigated by fracture toughness measurements

G. Aiello, C. Bonnekoh, A. Meier, T. Scherer, S. Schreck, K. Seemann, D. Strauss

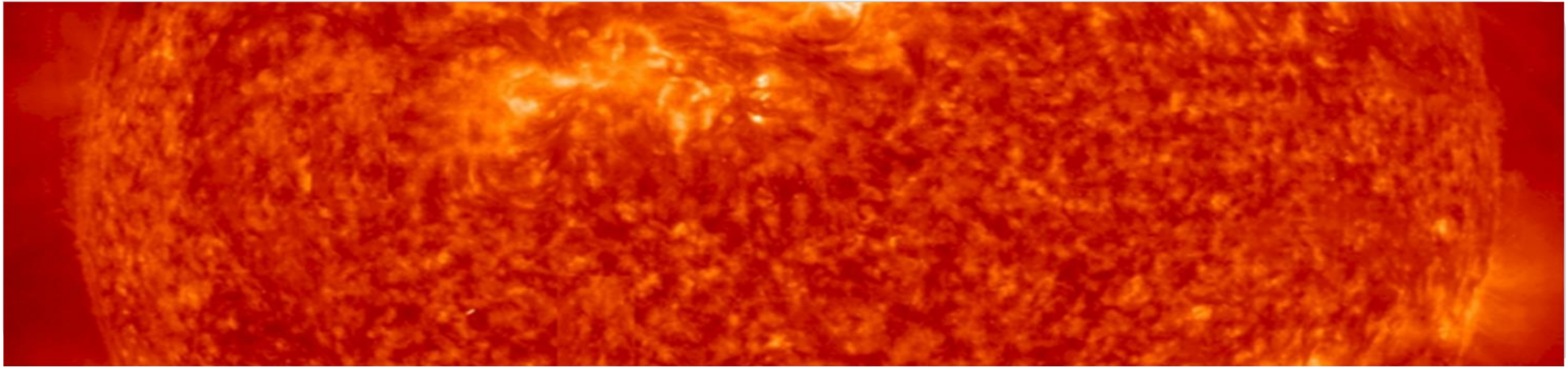

Outline

- Context
- MPA CVD diamond and properties
- Experimental setup for fracture toughness
- Characterization techniques for the samples
- Numerical analyses
- Summary and outlook

Context - EC H&CD system (ITER)

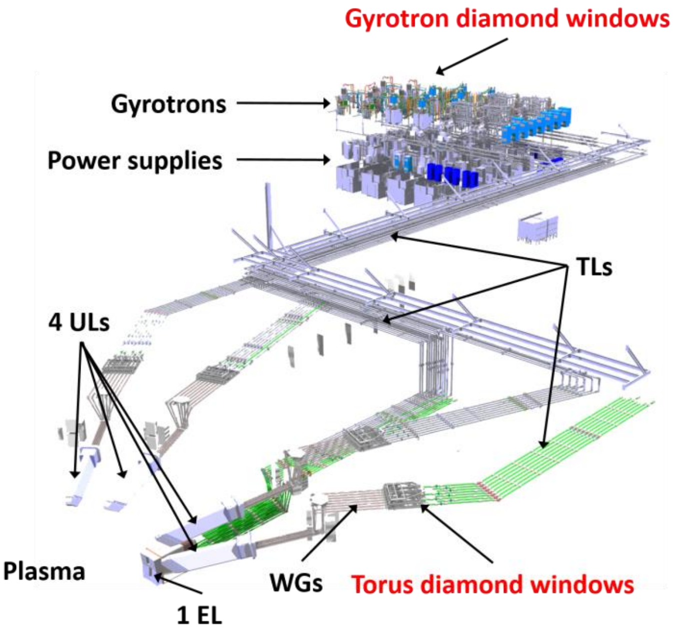

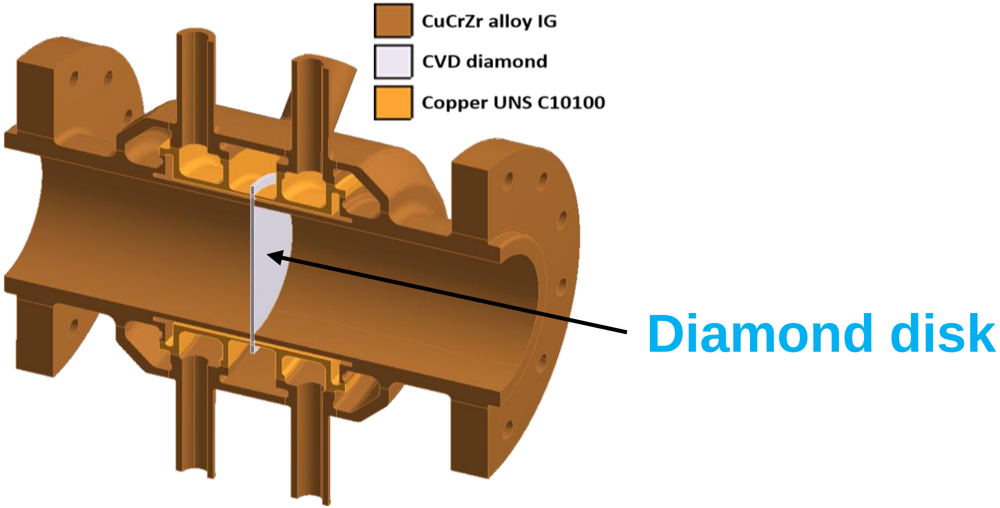

- Fundamental <u>safety role</u> of diamond disks in fusion reactors
- <u>Failure to fracture</u> is the main failure mode for the disks

MPA CVD diamond

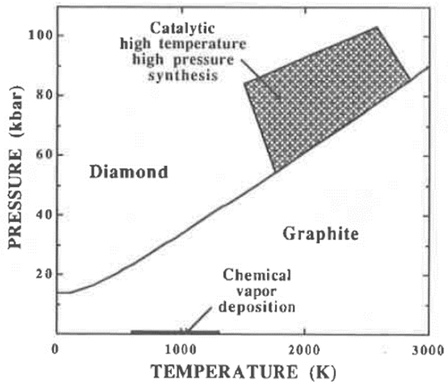

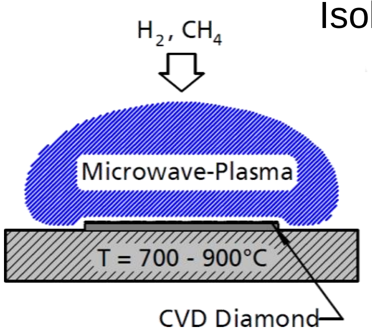

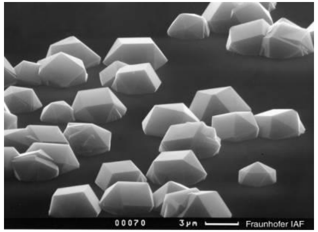

Isolated crystallites (nucleation)

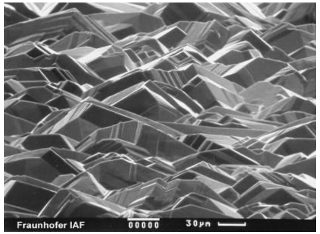

Polycrystalline plate

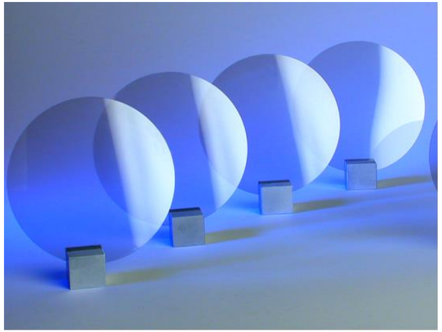

- Diamond growth by **Microwave Plasma Assisted (MPA) Chemical Vapour Deposition (CVD)**
- **Unique** solution for MW-class, CW operation
- Growth rate of 0.1-10 µm/h
- Disk **resonant** thickness t = 1.11 mm (ITER)

$$t = n\frac{\lambda_m}{2}$$

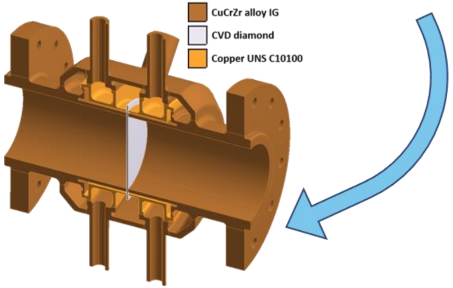

Fracture toughness (K_{IC}) of diamond - literature

Fracture toughness (MPa m$^{1/2}$)	Error (MPa m$^{1/2}$)	Type of diamond	Thickness (µm)	Shape	Dimensions (mm)	# of samples	Test method	Code	Papers no.	Year
6.3	**-**	**MPA CVD diamond**	**150 to 200**	**Disk**	**ø25**	**2**	**Tensile test**	**E-399**	**10, 1**	**1995**
5.6	**0.4**	**MPA CVD diamond**	**150 to 200**	**-**	**-**	**8**	**Indentation**		**10**	**1995**
5.3	**1.3**	**MPA CVD diamond**	**400**	**-**	**-**	**11**	**Indentation**		**6**	**1991**
8.7	**0.3**	**MPA CVD diamond**	**880**	**Rectangular**	**13 x 18**	**-**	**Double torsion**		**8**	**1998**
8.3	**0.4**	**MPA CVD optical diamond**	**1000**	**Rectangular**	**13 x 18**	**5**	**Double torsion**		**3**	**2004**
8.5	**1**	**MPA CVD mechanical diamond**	**1000**	**Rectangular**	**13 x 18**	**2**	**Double torsion**		**3**	**2004**
6.5	1.2	Arc-discharge CVD diamond	244 (aver.)	Disk	ø7 to ø16	5	Ball on ring		5	1992
7.6	1.8	Arc-discharge CVD diamond	244 (aver.)	Disk	-	4	Indentation		5	1992
8	-	Arc-discharge CVD diamond	485	Rectangular	2 x 10	9	Three-point	E-399	7	2000
9.2	-	Arc-discharge CVD diamond	485	Rectangular	2 x 10	8	Three-point	E-399	7	2000
4.6	-	Arc plasma jet CVD	300 to 700	Disk	ø8	-	Ball on ring		13	1998
6	-	CVD diamond	300	-	-	-	Indentation		2	1994
6.8	1.1	Arc plasma jet/hot filament CVD	450	Rectangular	2,5 x 12	3	Three-point	E-399	12	2001
3.4	-	Natural diamond type Ia and IIa	-	-	-	9	Indentation		4	1981
13	-	PDC - cobalt phase	700 (aver.)	Rectangular	~15 x 30	5	Double torsion		11	1994

Double torsion (DT) method for measurement

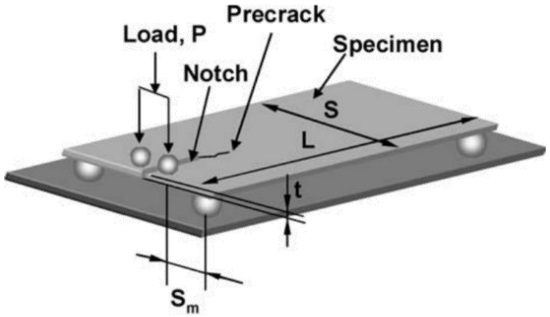

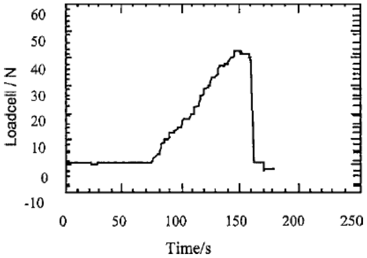

Plane strain

$$K = P S_m \left(\frac{3}{S t^4 (1-\nu)\psi} \right)^{1/2}$$

$$\psi = 1 - 0.6302\tau + 1.20\tau \exp(-\pi/\tau)$$

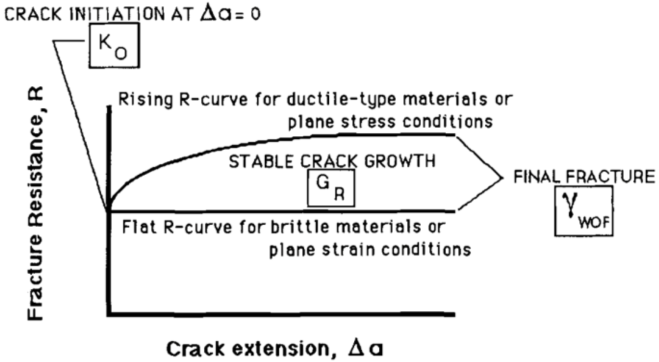

- Method applied to a very extensive range of materials
- However, it has not been standardized yet
- Key features:
  - A relatively simple method
  - K_I independent of crack lenght for a certain range
  - Ideal method for opaque materials

A. Shyam et al., J. Mater Sci 41, 2006

Diamond samples

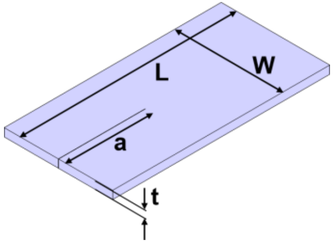

	t (mm)	W (mm)	L (mm)	L/W	W/t
Big samples	1.11	15	30	2.0	13.5
Small samples	1.11	12	22	1.8	10.8

- **Two diamond disks** fabricated at end 2023: optical and thermal grade
- **High cost** of diamond is the limiting factor for a good statistics in the experimental measurements
- **Preliminary** samples available for initial characterization

Thermal disk

ø 150 mm

Optical disk

ø 80 mm

Loss tangent measurements – optical grade

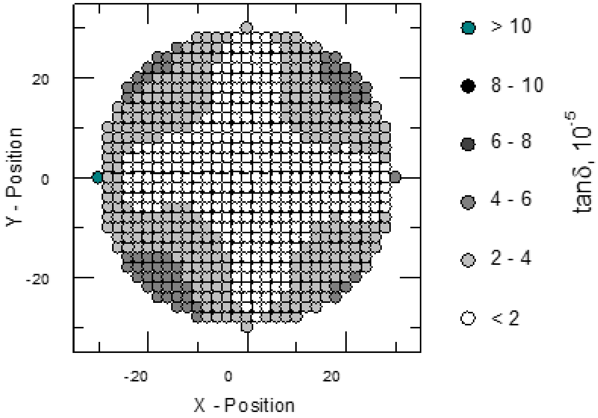

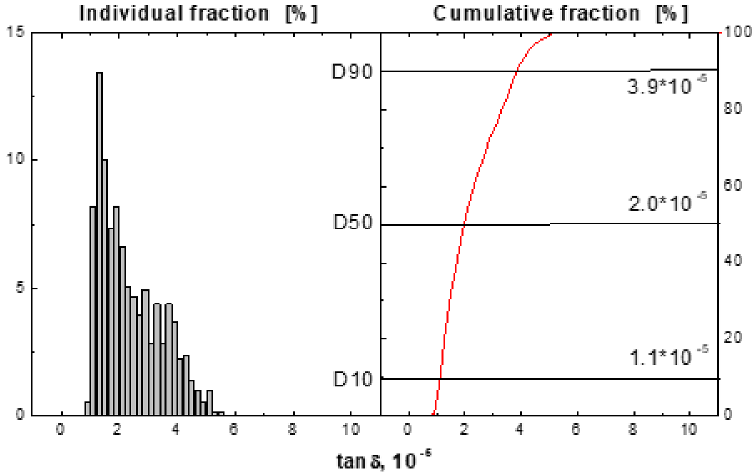

Hemispherical setup

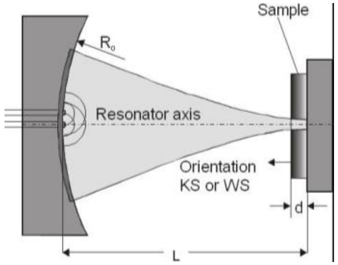

Acceptance criteria for ITER disks:

- $3.5x10^{-5}$ for the D50
- $6.0x10^{-5}$ for the D90

X-ray diffraction (XRD) measurements

Objectives:

- XRD pattern
- Texture measurements
- Residual stress analysis

Thermal quality | **Optical quality**

Growth Side (GS)

Nucleation Side (NS)

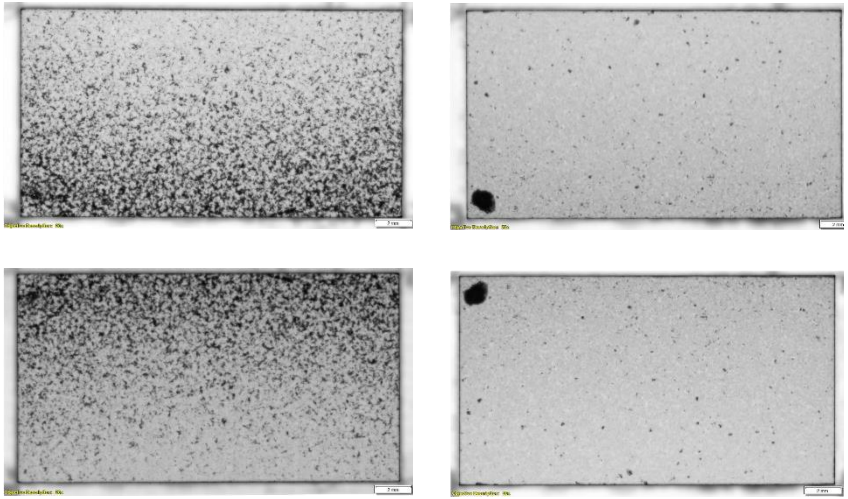

Empyrean diffractometer
(Malvern Panalytical)

XRD pattern – optical grade

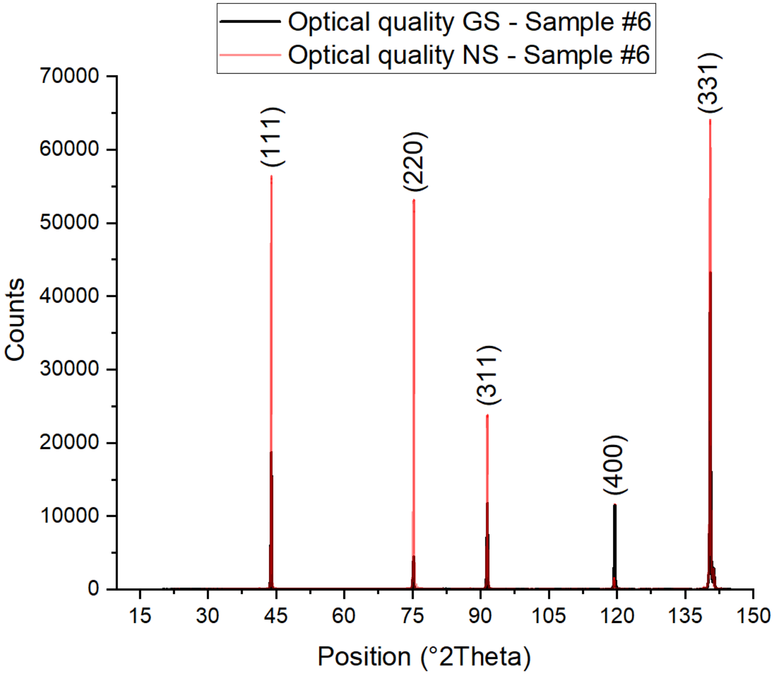

- The ratio of the peaks differs substantially from software database
- Different ratio of the peaks between GS and NS: a sign of a different texture in the sample surfaces

Database	
Planes	**I [%]**
111	**100**
220	**25**
311	**16**
400	**8**
331	**16**

Optical - GS	
Planes	**I [%]**
111	**100**
220	**24**
311	**63**
400	**62**
331	**232**

Optical - NS	
Planes	**I [%]**
111	**100**
220	**94**
311	**42**
400	**3**
331	**114**

XRD texture – optical quality

GS NS

111 Optical

111 Thermal

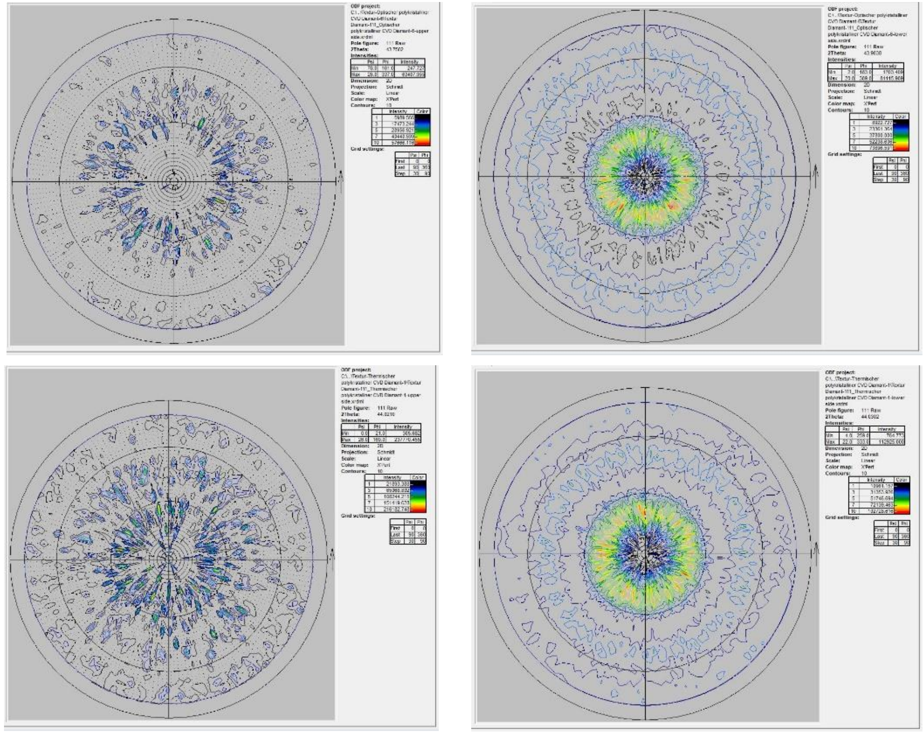

- Texture measurements were done in a 2 mm x 2 mm central area in the samples
- It was not possible to draw a clear conclusion
- No crystallographic direction is however perfectly parallel to the diamond growth direction
- As expected, circular symmetry occurs

→ Texture measurements to run by EBSD

XRD residual stress analysis - I

- Determination of macroscopic **in-plane** residual stresses by $\sin^2\Psi$ method
- Sampling area of 3 mm x 3 mm
- Cu K_α radiation
- (331) lattice plane selected corresponding to $2\theta = 140.6°$
- φ - 3 directions around surface normal
- Ψ - 16 sample tilt angles from 0 to 60°
- Modified Lorentzian shape function
- Isotropic elastic constants from database

$$\sigma_\phi = \left(\frac{E}{1+\nu}\right)_{(hkl)} \frac{1}{d_{\phi o}} \left(\frac{\partial d_{\varphi\psi}}{\partial \sin^2 \psi}\right)$$

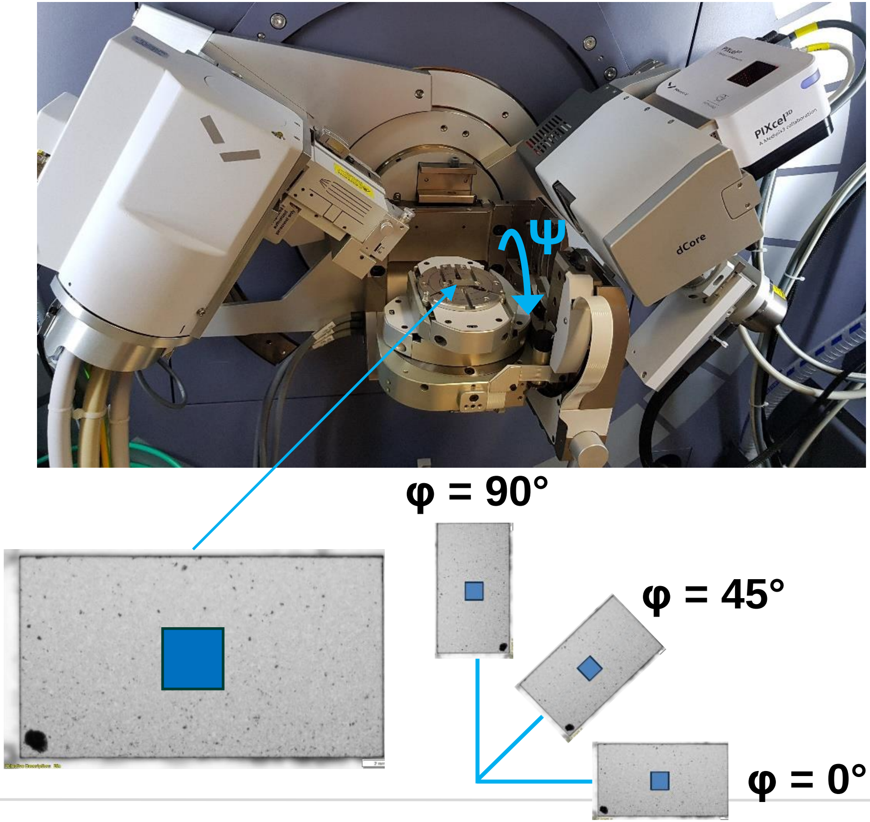

XRD residual stress analysis - II

- Determination of macroscopic **in-plane** residual stresses by $\sin^2\Psi$ method
- Sampling area of 3 mm x 3 mm
- Cu K_α radiation
- (331) lattice plane selected corresponding to 2θ = 140.6°
- φ - 3 directions around surface normal
- Ψ - 16 sample tilt angles from 0 to 60°
- Modified Lorentzian shape function
- Isotropic elastic constants from database

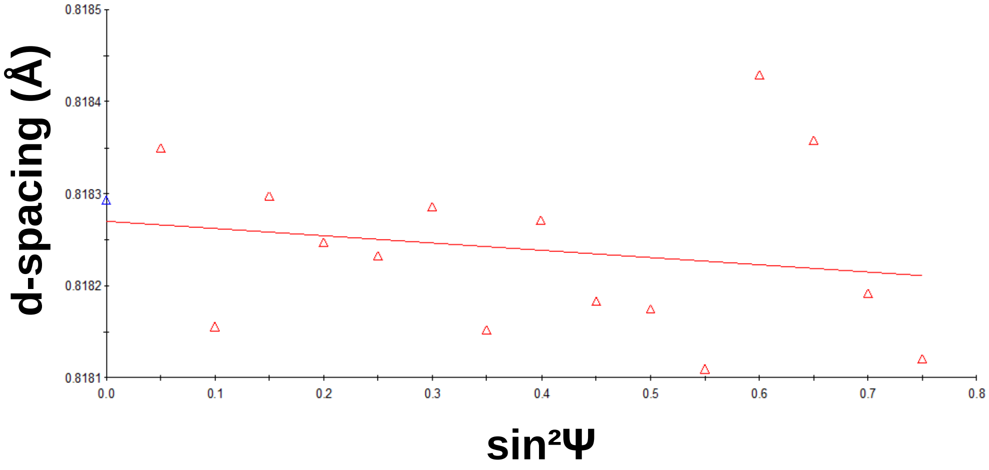

$$\sigma_\phi = \left(\frac{E}{1+v}\right)_{(hkl)} \frac{1}{d_{\phi o}} \left(\frac{\partial d_{\varphi\psi}}{\partial \sin^2 \psi}\right)$$

XRD residual stress analysis - III

Karlsruhe Institute of Technology

- First XRD residual stress measurements, to be consider as preliminary
- Average macro-residual stress appears to vary from few MPa to ~200 MPa, both in tensile and compression state
- Large value of standard deviation (maybe influence of texture, columnar growth as observed in Harker, 1994)
- Maybe triaxial stress state?
- Further investigations on the macro-residual stress state are ongoing

Optical grade

Φ (°)	GS σ (MPa)	NS σ (MPa)
0	74.7 ± 112	-8.8 ± 47.9
45	-114 ± 88.7	93.9 ± 45.9
90	-84.6 ± 110	-67.5 ± 34.6

Thermal grade

Φ (°)	GS σ (MPa)	NS σ (MPa)
0	-161 ± 88.6	25 ± 71.1
45	-26.9 ± 142	-47.2 ± 56.1
90	193 ± 122	-32.8 ± 90.5

Other characterization techniques

- **Raman**
  - Test measurements at ISSP, Riga (LV)
  - Measurements planned at KIT
- **Electron Backscatter Diffraction (EBSD)**
  - Data evaluation on going
- **Auger / XPS**
  - Measurements on going

Optical quality

Karlsruhe Institute of Technology

Numerical analyses - I

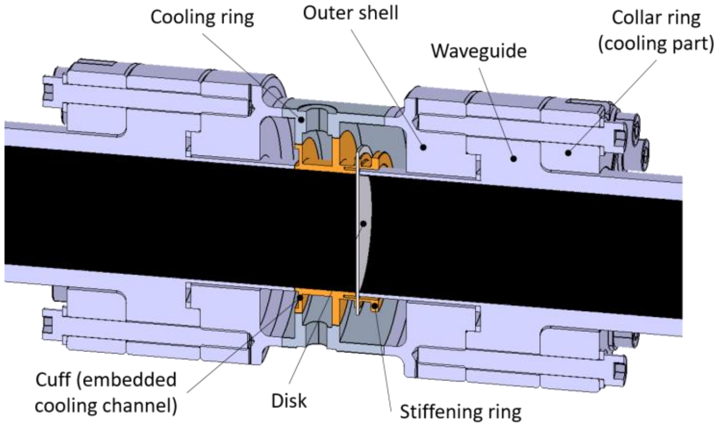

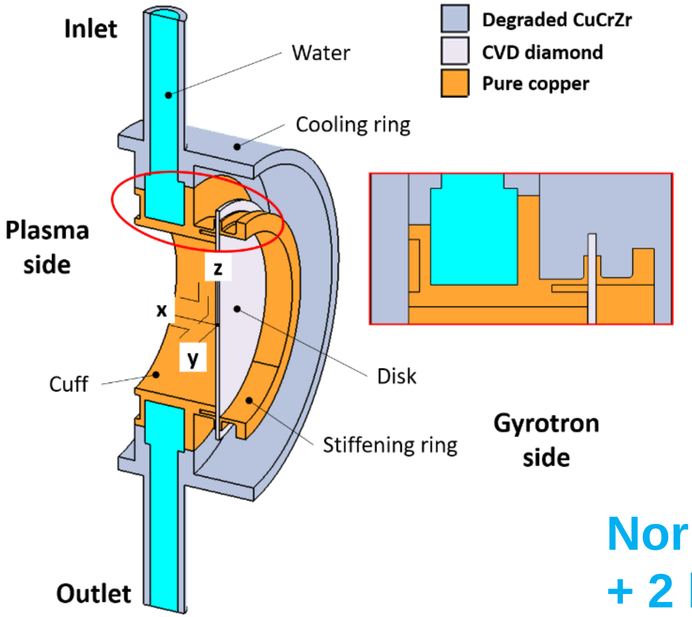

Normal Operation + 2 bar event

- HE_{11} beam power of 1.31 MW
- Symmetry
- 5.22 l/min and 30°C at inlet
- 0 Pa at outlet

- Disk tanδ = 2.0E-5
- Disk thickness = 1.11 mm
- P_{abs} = 346 W
- Heat flux at cuff = 3882 W m^{-2}

$$P_{abs} = P_{beam} \cdot \frac{f}{c} \cdot \pi \cdot (1+\varepsilon_r) \cdot \tan\delta \cdot t$$

Numerical analyses - II

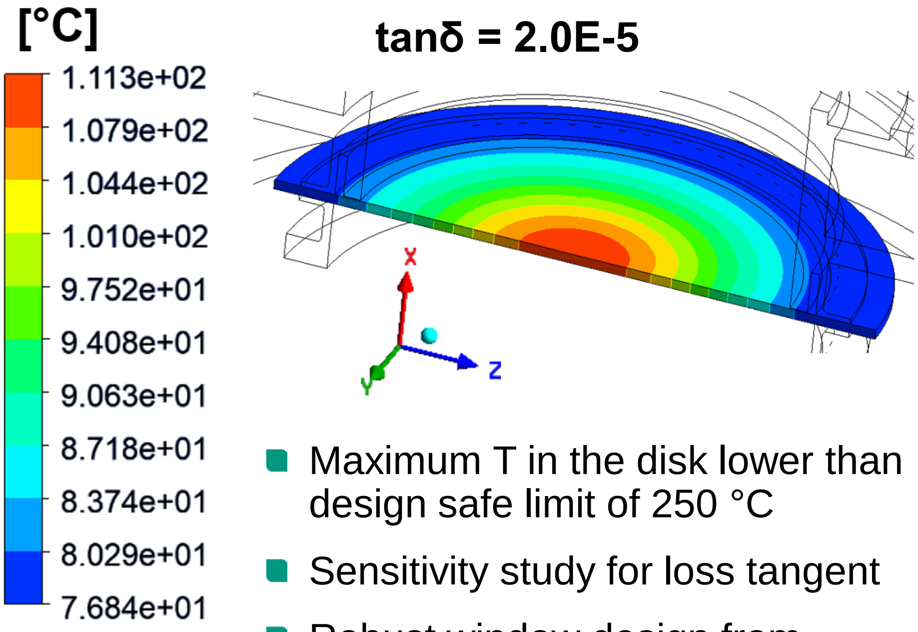

- Maximum T in the disk lower than design safe limit of 250 °C
- Sensitivity study for loss tangent
- Robust window design from thermal perspective

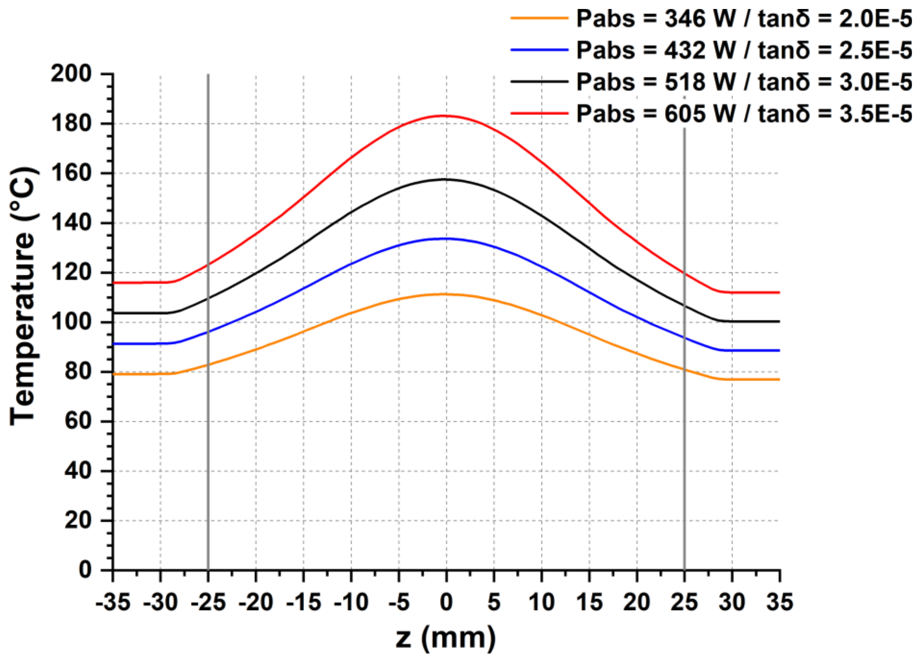

Numerical analyses - III

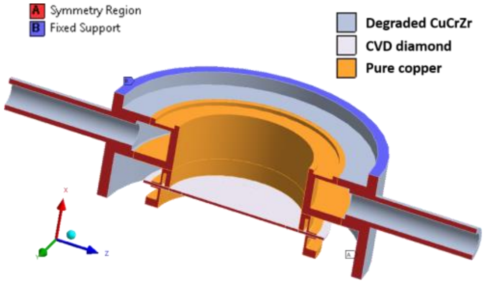

- Worst case: Normal Operation + 2 bar event on cuff side
- Maximum stress in the disk lower than 150 MPa allowable limit
- Vector plots of the maximum principal stresses

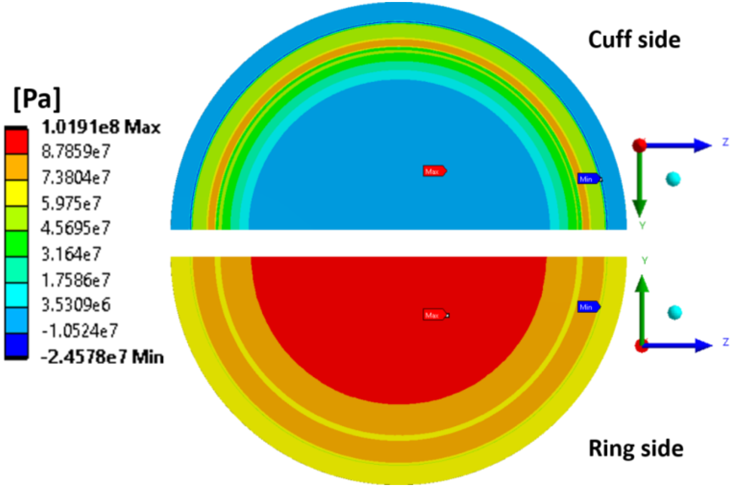

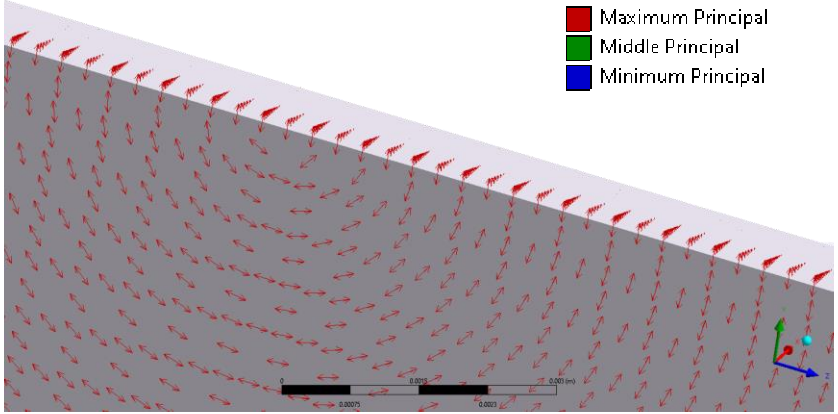

Summary & outlook

- A deeper mechanical characterization of MPA CVD diamond regarding its main failure mode is required
- The method for fracture toughness measurement was selected and characterization of the diamond samples have been started
- Numerical analyses for worst load scenario of the diamond disks were performed

- Continue characterization of samples
- Generate drawings of the setup and carry out the experiments

This work was supported by Fusion for Energy (F4E) under the grant contract No. F4E-GRT-615. The views and opinions expressed herein reflect only the author’s views and not necessarily those of F4E and ITER Organisation (IO). F4E and IO are not liable for any use that may be made of the information contained therein.

This work has been carried out within the framework of the EUROfusion Consortium, funded by the European Union via the Euratom Research and Training Programme (Grant Agreement No 101052200 — EUROfusion). Views and opinions expressed are however those of the author(s) only and do not necessarily reflect those of the European Union or the European Commission. Neither the European Union nor the European Commission can be held responsible for them.